Kinetic and Related Models
©American Institute of Mathematical Sciences
Volume **13**, Number **4**, August **2020**
doi:10.3934/krm.2020023
pp. **677–702**

A PETROV-GALERKIN SPECTRAL METHOD FOR THE INELASTIC BOLTZMANN EQUATION USING MAPPED CHEBYSHEV FUNCTIONS

Jingwei Hu* and Jie Shen

Department of Mathematics, Purdue University, West Lafayette, IN 47907 USA

Yingwei Wang

SAS Institute, Inc., Cary, NC 27513 USA

(Communicated by Lorenzo Pareschi)

Abstract. We develop in this paper a Petrov-Galerkin spectral method for the inelastic Boltzmann equation in one dimension. Solutions to such equations typically exhibit heavy tails in the velocity space so that domain truncation or Fourier approximation would suffer from large truncation errors. Our method is based on the mapped Chebyshev functions on unbounded domains, hence requires no domain truncation. Furthermore, the test and trial function spaces are carefully chosen to obtain desired convergence and conservation properties. Through a series of examples, we demonstrate that the proposed method performs better than the Fourier spectral method and yields highly accurate results.

1. **Introduction.** Since the beginning of 1990s, significant attention has been devoted to modeling of granular materials, e.g., sand, powders, grains, snow, or even asteroids. Among the main motivations are the need for new insights concerning how granular materials behave under shaking, how flows are evolving or how to prevent them, how to facilitate mixing, how matter aggregates in a newborn solar system, etc. At the kinetic level, granular materials can be described by the so-called inelastic Boltzmann equation [14, 1, 11, 2], wherein particles interact like hard spheres but with some energy loss. Recently, the inelastic Boltzmann equation has also been used in the modeling of social and biological systems, see [35].

This paper is devoted to the development of efficient spectral methods for inelastic kinetic models. Specifically, we will focus on the following one-dimensional spatially homogeneous Boltzmann equation:

$$\frac{\partial f}{\partial t} = Q^{e,\lambda}(f,f)(v), \quad t > 0, \quad v \in \mathbb{R}, \tag{1}$$

2010 *Mathematics Subject Classification.* Primary: 65M70, 35Q20, 41A50; Secondary: 65R20.

Key words and phrases. Inelastic Boltzmann equation, heavy tail, granular material, Petrov-Galerkin spectral method, mapped Chebyshev function, unbounded domain.

J. Hu's research was supported by NSF grant DMS-1620250 and NSF CAREER grant DMS-1654152. J. Shen's research was supported in part by NSF DMS-1720442 and AFOSR FA9550-16-1-0102.

* Corresponding author: Jingwei Hu.

where $f = f(v,t)$ represents the probability density of particles at time t with velocity v, and $Q^{e,\lambda}(f,f)$ is a quadratic integral operator modeling binary collisions among particles. The operator $Q^{e,\lambda}(f,f)$ is most conveniently written in the following weak form:

$$\begin{aligned}&\int_{\mathbb{R}} Q^{e,\lambda}(f,f)(v)\phi(v)\,\mathrm{d}v\\ =&\frac{1}{2}\iint_{\mathbb{R}^2} B_\lambda(|v-w|)f(v)f(w)\left[\phi(v')+\phi(w')-\phi(v)-\phi(w)\right]\mathrm{d}v\,\mathrm{d}w,\end{aligned} \tag{2}$$

where $\phi \in C(\mathbb{R})$ is a test function. (v,w) and (v',w') are the velocities of two particles before and after a collision, defined as

$$v' = \frac{1}{2}(v+w) + \frac{e}{2}(v-w), \quad w' = \frac{1}{2}(v+w) - \frac{e}{2}(v-w), \tag{3}$$

with $0 \le e \le 1$ being the restitution coefficient. Note that perfectly elastic (resp., inelastic) collisions correspond to the case $e = 1$ (resp., $e = 0$) and partially inelastic collisions are obtained if $e \in (0,1)$. In fact, from (3), one can easily derive that

$$v' + w' = v + w; \quad v'^2 + w'^2 - v^2 - w^2 = -\frac{1-e^2}{2}(v-w)^2 \le 0, \tag{4}$$

which implies the momentum is always conserved while the energy is dissipative. Finally the function B_λ in (2) is the collision kernel, given by

$$B_\lambda = C_\lambda |v-w|^\lambda, \tag{5}$$

where $0 \le \lambda \le 1$ characterizes the strength of particle interactions and C_λ is some positive constant. The case $\lambda = 1$ corresponds to hard spheres and $\lambda = 0$ corresponds to Maxwell molecules.

There are several interesting features of the inelastic model considered above, compared to the perfectly elastic ones (indeed the collision operator is trivial in 1D when $e = 1$), such as non-Maxwellian equilibrium states, finite time energy extinction, quasi-elastic asymptotics, large-time behaviors and so on, see for example, the studies in [5, 12, 39, 4], also the review papers [41, 13] and the references therein. Numerically, mainly two classes of methods have been considered for the inelastic Boltzmann equation, one stochastic and one deterministic. The direct simulation Monte Carlo (DSMC) method, due to its simplicity and efficiency, is historically popular and still quite appealing nowadays for full 3D simulations [25, 36]. On the other hand, as the computing power grows, the deterministic methods have received a lot of attention in the past decade, among which the spectral methods based on Fourier series/transform constitute the mainstream thanks to their high accuracy and relatively low computational complexity [32, 19, 26, 20, 45, 27]. Nevertheless, compared to their success for elastic Boltzmann equations [33, 8, 34, 21, 31, 18, 26, 17, 28, 44, 22], the Fourier spectral method does not seem to be the optimal choice for the inelastic equation, especially for long time steady state calculation. It is well-known that the quality of Fourier approximation depends heavily on the support of the approximated function, due to the truncation from unbounded domain $\mathbb{R}$ to a finite one $[-L, L]$. If the approximated function is a Gaussian, as is typical for the solution to the elastic Boltzmann equation, then the errors from truncation of the domain can be negligible as long as L is chosen large enough. However, the solution to the inelastic Boltzmann equation is usually far from Gaussian distributions. Actually, the steady state of (1) is the Dirac delta function. Using a velocity rescaling technique, one can show that the

distribution function, in the case of Maxwell molecules, has an algebraic tail like $|v|^{-4}$ for $|v| \to \infty$, see [1, 7]. Furthermore, if a driving mechanism, say, thermal bath, is added to the system (to prevent energy loss, as is done in many experiments of granular materials), the steady state solution would also exhibit heavy tails like $\exp(-a|v|^b)$ with $1 \le b \le 3/2$ as $|v| \to \infty$, see [40, 6, 23]. In either of these two cases, one needs a much larger computational domain than that for Gaussians in order to capture the solution accurately. Another problem associated with the Fourier spectral method for both the elastic and inelastic Boltzmann equations is that momentum and energy conservation properties can not be easily satisfied (the energy can be conserved in the inelastic case if a velocity rescaling technique is applied, see Section 2.1). These issues motivate us to seek an alternative approach.

In this paper, we develop a spectral method for the inelastic Boltzmann equation (1) using mapped Chebyshev functions on unbounded domains [9, 38], in which no domain truncation is required. Yet, since the solution of (1) converges to zero as $|v| \to \infty$, the space of trial functions can not include any polynomials such as 1, v, v^2. Therefore, a Galerkin approach, with test space being the same as trial space, will not be able to conserve or well approximate physically important quantities such as mass, momentum and energy. This leads us to develop a Petrov-Galerkin approach, for both the velocity rescaling case and the heated case, in which test functions are carefully chosen so that the mass, momentum and energy can be automatically conserved or well approximated. Therefore, our proposed method enjoys the following merits: (i) There is no domain truncation so no need to set any artificial boundary conditions; (ii) The method is of Petrov-Galerkin type with test and trial functions chosen carefully to achieve the desired convergence and conservation properties; (iii) The mapped Chebyshev polynomials have excellent approximation properties and are amenable to fast Fourier transforms thanks to their close relations to Fourier series [30].

Our discussion in this paper is limited to the one-dimensional case since our main purpose here is to demonstrate the better approximation properties of the proposed mapped Chebyshev bases compared to Fourier basis. We mention that there are several recent works [24, 29, 42] which propose different spectral approximations to the Boltzmann equation (using Hermite polynomials, etc.). While these methods can achieve better approximation property than Fourier, to the best of our knowledge, there does not exist any fast algorithm (at least with a similar complexity as the Fourier spectral method). Our framework, however, has the potential to be accelerated by the nonuniform fast Fourier transform. Some perspectives are given at the end of the paper and constitute our ongoing work.

The remaining sections are organized as follows. In Section 2, we summarize briefly the properties of the inelastic Boltzmann equation. In Section 3, we introduce the mapped Chebyshev approximation and describe in detail our proposed Petrov-Galerkin spectral method. Approximation property for the function and conservation property for the moments are proved as well. In Section 4, we present several numerical examples to demonstrate the accuracy of the new method. Finally, Section 5 contains some concluding remarks.

2. **The inelastic Boltzmann equation and its basic properties.**

In this section, we briefly summarize the basic properties of the inelastic Boltzmann equation (1) and focus in particular on its long time asymptotics.

First of all, it is sometimes convenient to use an alternative weak form of the Boltzmann equation:

$$\frac{\partial}{\partial t}\int_{\mathbb{R}} f\phi \,\mathrm{d}v = \iint_{\mathbb{R}^2} B_\lambda(|v-w|)f(v)f(w)\left[\phi(v')-\phi(v)\right]\,\mathrm{d}v\,\mathrm{d}w, \tag{6}$$

which can be derived from (2) by a simple change of variables (swap v and w, hence v' and w' due to (3), in the second and fourth terms in the bracket of (2)).

Define the moments of f as

$$\rho = \int_{\mathbb{R}} f\,\mathrm{d}v, \quad m = \rho u = \int_{\mathbb{R}} fv\,\mathrm{d}v, \quad E = \frac{1}{2}\rho u^2 + \frac{1}{2}\rho T = \int_{\mathbb{R}} f\frac{v^2}{2}\,\mathrm{d}v, \tag{7}$$

where ρ is the density, m is the momentum, u is the bulk velocity, E is the total energy, and T is the temperature. Then taking the moments $\int_{\mathbb{R}} \cdot (1, v, v^2/2)^T\,\mathrm{d}v$ on both sides of (1), we obtain

- conservation of mass

$$\frac{\partial \rho}{\partial t} = \int_{\mathbb{R}} Q^{e,\lambda}(f,f)\,\mathrm{d}v = 0; \tag{8}$$

- conservation of momentum

$$\frac{\partial m}{\partial t} = \int_{\mathbb{R}} Q^{e,\lambda}(f,f)v\,\mathrm{d}v = 0; \tag{9}$$

- dissipation of energy

$$\frac{\partial E}{\partial t} = \int_{\mathbb{R}} Q^{e,\lambda}(f,f)\frac{v^2}{2}\,\mathrm{d}v = -\frac{1-e^2}{8}\iint_{\mathbb{R}^2} B_\lambda(|v-w|)f(v)f(w)(v-w)^2\,\mathrm{d}v\,\mathrm{d}w \le 0, \tag{10}$$

where we used the weak form (2) by choosing $\phi = 1, v, v^2/2$ and the relation (4).

Equations (8)-(10) imply that if $e < 1$, the temperature of the system will decrease to zero and the solution will eventually approach a Dirac delta function $\rho\,\delta(v-u)$.

2.1. **A velocity rescaling technique.** To better study the long time behavior of the system, a standard way is to look for a self-similar solution by rescaling the velocity as (see for instance [13])

$$\tilde{v} = \frac{v}{\sqrt{T(t)}}, \quad g(\tilde{v},t) = \sqrt{T(t)}f(v,t). \tag{11}$$

Without loss of generality, we assume the initial data satisfies

$$\rho_0 = 1, \quad u_0 = 0, \quad T_0 = 1. \tag{12}$$

Then for the new function g, one has

$$\int_{\mathbb{R}} g\,\mathrm{d}\tilde{v} \equiv 1, \quad \int_{\mathbb{R}} g\tilde{v}\,\mathrm{d}\tilde{v} \equiv 0, \quad \int_{\mathbb{R}} g\tilde{v}^2\,\mathrm{d}\tilde{v} \equiv 1, \tag{13}$$

i.e., its temperature is a fixed constant 1. Furthermore, it can be derived from (6) that $g(\tilde{v},t)$ satisfies the following equation

$$\begin{aligned}\frac{\partial}{\partial t}&\int_{\mathbb{R}} g\phi\,\mathrm{d}\tilde{v}\\ &= -\frac{1}{2}T^{-1}\frac{\partial T}{\partial t}\int_{\mathbb{R}} \tilde{v}g\frac{\partial \phi}{\partial \tilde{v}}\,\mathrm{d}\tilde{v} + \iint_{\mathbb{R}^2} B_\lambda(\sqrt{T}|\tilde{v}-\tilde{w}|)g(\tilde{v})g(\tilde{w})[\phi(\tilde{v}')-\phi(\tilde{v})]\,\mathrm{d}\tilde{v}\,\mathrm{d}\tilde{w}.\end{aligned} \tag{14}$$

For Maxwell molecules ($\lambda = 0$ in (5)), if we assume $C_0 = 1$, the above equation becomes (dropping $\sim$ for simplicity)

$$\frac{\partial}{\partial t}\int_{\mathbb{R}} g\phi \,\mathrm{d}v = -\frac{1}{2}T^{-1}\frac{\partial T}{\partial t}\int_{\mathbb{R}} vg\frac{\partial \phi}{\partial v}\,\mathrm{d}v + \iint_{\mathbb{R}^2} g(v)g(w)[\phi(v') - \phi(v)]\,\mathrm{d}v\,\mathrm{d}w. \quad (15)$$

On the other hand, for initial data (12) and Maxwell molecules, (10) reduces to

$$\frac{\partial T}{\partial t} = -\frac{1-e^2}{2}T. \quad (16)$$

Applying this in (15), one obtains

$$\frac{\partial}{\partial t}\int_{\mathbb{R}} g\phi \,\mathrm{d}v = \frac{1-e^2}{4}\int_{\mathbb{R}} vg\frac{\partial \phi}{\partial v}\,\mathrm{d}v + \iint_{\mathbb{R}^2} g(v)g(w)[\phi(v') - \phi(v)]\,\mathrm{d}v\,\mathrm{d}w. \quad (17)$$

Compared to (6), the function g satisfies a similar inelastic Boltzmann equation but with a drift term.

Using the Fourier transform of (17) (in the velocity variable), it can be shown that [1, 7]:

1. if $e = 1$, the steady state is the Maxwellian function

$$g(v, t = \infty) = M_0(v) = \frac{1}{\sqrt{2\pi}}\exp\left\{-\frac{v^2}{2}\right\}; \quad (18)$$

2. if $e < 1$, the steady state is the Lorentz function

$$g(v, t = \infty) = M_1(v) = \frac{2}{\pi(1+v^2)^2}. \quad (19)$$

2.2. **The heated inelastic Boltzmann equation.** Many experiments about granular materials include shaking, as a way to input energy into the system, counterbalancing the freezing due to energy loss. Mathematically, this amounts to adding to the right hand side of the equation (1) a diffusion term [43, 3]:

$$\frac{\partial f}{\partial t} = Q^{e,\lambda}(f,f)(v) + \varepsilon\frac{\partial^2 f}{\partial v^2}, \quad t > 0, \quad v \in \mathbb{R}, \quad (20)$$

where $0 \le \varepsilon \le 1$ is a small diffusion coefficient. The weak form of this equation is

$$\frac{\partial}{\partial t}\int_{\mathbb{R}} f\phi\,\mathrm{d}v = \iint_{\mathbb{R}^2} B_\lambda(|v-w|)f(v)f(w)\left[\phi(v') - \phi(v)\right]\,\mathrm{d}v\,\mathrm{d}w - \varepsilon\int_{\mathbb{R}}\frac{\partial f}{\partial v}\frac{\partial \phi}{\partial v}\,\mathrm{d}v, \quad (21)$$

from which one can still derive the conservation of mass and momentum. The equation for energy becomes

$$\frac{\partial E}{\partial t} = -\frac{1-e^2}{8}\iint_{\mathbb{R}^2} B_\lambda(|v-w|)f(v)f(w)(v-w)^2\,\mathrm{d}v\,\mathrm{d}w + \varepsilon\rho. \quad (22)$$

If we consider again the initial data (12), and Maxwell molecules such that $C_0 = 1$, then the above equation reduces to

$$\frac{\partial T}{\partial t} = -\frac{1-e^2}{2}T + 2\varepsilon. \quad (23)$$

Therefore, the temperature evolution is given by

$$T(t) = \left(T_0 - \frac{4\varepsilon}{1-e^2}\right)\exp\left\{-\frac{1-e^2}{2}t\right\} + \frac{4\varepsilon}{1-e^2}. \quad (24)$$

This analytical formula can be used to validate the accuracy of the numerical solution. See Section 4.2.3.

The asymptotic behavior of the steady state solution to the heated inelastic Boltzmann equation (20) has been studied in many works [6, 40, 23]. In particular, it was shown that

1. for Maxwell molecules ($\lambda = 0$), the steady state behaves asymptotically as
$$f(v, t = \infty) \sim M_2(v) = \exp(-a|v|), \quad |v| \to \infty; \tag{25}$$
2. for hard spheres ($\lambda = 1$), the steady state behaves asymptotically as
$$f(v, t = \infty) \sim M_3(v) = \exp(-a|v|^{3/2}), \quad |v| \to \infty. \tag{26}$$

3. **Mapped Chebyshev spectral methods.** From the previous section, we have seen that the typical solutions to the inelastic Boltzmann equation are very different from Gaussians. Due to their heavy velocity tails, it is expected that the Fourier approximation, which requires the truncation of an infinite domain into a bounded one, will not yield the optimal result. To deal with unbounded domains, popular spectral methods include Hermite functions, rational functions through mapped Jacobi functions, etc. [9, 37, 15, 47]. In this section, we will employ the mapped Chebyshev functions in [38] to construct a Petrov-Galerkin spectral method for the inelastic Boltzmann equation.

To this end, we first introduce two kinds of mapped Chebyshev functions, which will be used later as bases for trial functions and test functions, respectively. Then we describe in detail the proposed Petrov-Galerkin spectral method for the inelastic Boltzmann equation including both the rescaled case (17) and the heated case (21). The approximation property for the function and conservation property for the moments are carried out later.

3.1. **Mapped Chebyshev functions and useful properties.** First, let us define the inner product $(\cdot,\cdot)_\omega$ on $I = (-1, 1)$ and $(\cdot,\cdot)_{\mathbb{R}}$ on $\mathbb{R}$ respectively by
$$(U, W)_\omega = \int_I \omega(\xi)U(\xi)W(\xi)\mathrm{d}\xi, \quad (u, w)_{\mathbb{R}} = \int_{\mathbb{R}} u(v)w(v)\mathrm{d}v, \tag{27}$$
where the weight function $\omega(\xi)$ is given by
$$\omega(\xi) = (1 - \xi^2)^{-1/2}. \tag{28}$$

Next, let us consider the one-to-one mapping $v = v(\xi) : I \to \mathbb{R}$, satisfying
$$\frac{\mathrm{d}v}{\mathrm{d}\xi} = \frac{S}{(1 - \xi^2)^{1+r/2}} = \frac{\omega(\xi)}{[\mu(\xi)]^2}, \quad v(\pm 1) = \pm\infty, \tag{29}$$
where $S > 0$ is the scaling parameter, $r \geq 0$ is the tail parameter, $\omega(\xi)$ is defined by (28) and the function $\mu(\xi)$ is defined as
$$\mu(\xi) = \frac{(1 - \xi^2)^{(1+r)/4}}{\sqrt{S}}, \quad \xi \in I = (-1, 1). \tag{30}$$

Hereafter, the function pair $u(v)$ and $U(\xi)$ satisfy
$$u(v) \equiv U(\xi), \quad v \in \mathbb{R},\ \xi \in I, \tag{31}$$
where the mapping $v(\xi)$ is determined by (29). Moreover, suppose both $u(v), U(\xi)$ and $w(v), W(\xi)$ satisfy the relation (31), then we have
$$(u, w)_{\mathbb{R}} = (\mu^{-2}U, W)_\omega, \quad (U, W)_\omega = (\mu^2 u, w)_{\mathbb{R}}. \tag{32}$$

To simplify the notations, we use μ to denote both $\mu(\xi)$ and $\mu(\xi(v))$.

Recall that the Chebyshev polynomials $\{T_k(\xi)\}_{k=0}$ on the interval I are orthogonal with respect to the weight $\omega(\xi)$, i.e.,

$$(T_k, T_j)_\omega = \int_{-1}^{1} T_k(\xi)T_j(\xi)\omega(\xi)\mathrm{d}\xi = c_k\delta_{kj}, \tag{33}$$

where $c_0 = \pi,\ c_k = \pi/2$ for $k \geq 1$.

By (32) and (33), we have the following orthogonal relation:

$$\int_{\mathbb{R}} [\mu(\xi(v))]^2 \frac{T_k(\xi(v))}{\sqrt{c_k}} \frac{T_j(\xi(v))}{\sqrt{c_j}} \mathrm{d}v = \frac{1}{\sqrt{c_k c_j}} \int_{-1}^{1} T_k(\xi)T_j(\xi)\omega(\xi)\mathrm{d}\xi = \delta_{kj}. \tag{34}$$

We consider two sets of mapped Chebyshev functions on $\mathbb{R}$: $\hat{\mathbb{T}}_N = \{\hat{T}_k(v)\}_{k=0}^N$ and $\tilde{\mathbb{T}}_N = \{\tilde{T}_k(v)\}_{k=0}^N$ defined by

$$\hat{T}_k(v) := \frac{[\mu(\xi(v))]^{-2}}{\sqrt{c_k}} T_k(\xi(v)), \quad \forall \hat{T}_k \in \hat{\mathbb{T}}_N, \tag{35}$$

$$\tilde{T}_k(v) := \frac{[\mu(\xi(v))]^{4}}{\sqrt{c_k}} T_k(\xi(v)), \quad \forall \tilde{T}_k \in \tilde{\mathbb{T}}_N, \tag{36}$$

where $v \in (-\infty, +\infty)$ and $\xi(v)$ is determined by (29). Thanks to (34), we have

$$\left(\tilde{T}_k, \hat{T}_j\right)_{\mathbb{R}} = \frac{1}{\sqrt{c_k c_j}} (T_k, T_j)_\omega = \delta_{kj}, \quad \forall \tilde{T}_k \in \tilde{\mathbb{T}}_N, \hat{T}_j \in \hat{\mathbb{T}}_N. \tag{37}$$

Suppose $u(v)$ can be expanded by $\{\tilde{T}_k(v)\}_{k=0}^\infty$, i.e.,

$$u(v) = \sum_{k=0}^{\infty} \tilde{u}_k [\mu(\xi(v))]^4 \frac{T_k(\xi(v))}{\sqrt{c_k}} = \sum_{k=0}^{\infty} \tilde{u}_k \tilde{T}_k(\xi(v)). \tag{38}$$

Then the expansion coefficients $\{\tilde{u}_k\}_{k=0}^\infty$ are determined by

$$\begin{aligned} \tilde{u}_k &= \left(u, \hat{T}_k\right)_{\mathbb{R}} = \int_{\mathbb{R}} u(v)\hat{T}_k(v)\mathrm{d}v \\ &= \frac{1}{\sqrt{c_k}} \int_{-1}^{1} \frac{U(\xi)}{[\mu(\xi)]^4} T_k(\xi)\omega(\xi)\mathrm{d}\xi = \frac{1}{\sqrt{c_k}} \left(\mu^{-4}U, T_k\right)_\omega. \end{aligned} \tag{39}$$

Note that the Chebyshev transform shown in (39) can be performed in $O(N \log N)$ operations via FFTs in general.

Two useful examples for the mapping between $v \in (-\infty, \infty)$ and $\xi \in (-1, 1)$ defined by (29) are $r = 0$ and $r = 1$, which can be explicitly written as follows

(1) logarithmic mapping ($r = 0$):

$$v = \frac{S}{2} \ln\left(\frac{1+\xi}{1-\xi}\right), \quad \xi = \tanh\left(\frac{v}{S}\right), \quad \text{with } \mu(\xi) = \frac{1}{\sqrt{S}}(1-\xi^2)^{1/4}; \tag{40}$$

(2) algebraic mapping ($r = 1$):

$$v = \frac{S\xi}{\sqrt{1-\xi^2}}, \quad \xi = \frac{v}{\sqrt{S^2+v^2}}, \quad \text{with } \mu(\xi) = \frac{1}{\sqrt{S}}(1-\xi^2)^{1/2}. \tag{41}$$

Note that in the Petrov-Galerkin method to be described in Section 3.2, we use $\tilde{\mathbb{T}}_N$ as the set of *trial* functions while $\hat{\mathbb{T}}_N$ as the set of *test* functions. Next, we derive some useful properties related to these two mapped Chebyshev function sets.

Lemma 3.1 (Decay property of $\{\tilde{T}_k\}$ and increase property of $\{\hat{T}_k\}$)**.** *For any $k \geq 0$ and $|v| \gg 1$, we have*

$$|\tilde{T}_k(v)| \sim \begin{cases} \mathrm{e}^{-2|v|}, & r = 0, \\ |v|^{-4}, & r = 1; \end{cases} \tag{42}$$

$$|\hat{T}_k(v)| \sim \begin{cases} \mathrm{e}^{|v|}, & r = 0, \\ |v|^{2}, & r = 1. \end{cases} \tag{43}$$

Proof. It is easy to know that

$$\lim_{|v|\to\infty} |T_k(\xi(v))| = 1, \quad \forall k = 0, 1, \ldots. \tag{44}$$

It follows that

$$\lim_{|v|\to\infty} |\tilde{T}_k(v)| \sim \lim_{|v|\to\infty} [\mu(\xi(v))]^4, \tag{45}$$

$$\lim_{|v|\to\infty} |\hat{T}_k(v)| \sim \lim_{|v|\to\infty} [\mu(\xi(v))]^{-2}. \tag{46}$$

Setting $S = 1$ in (40) and (41), respectively, leads to

$$r = 0, \qquad \mu^2 = (1-\xi^2)^{1/2} = \operatorname{sech}(v) \sim \mathrm{e}^{-|v|}, \tag{47}$$

$$r = 1, \qquad \mu^2 = 1 - \xi^2 = \frac{1}{1+v^2} \sim |v|^{-2}, \tag{48}$$

as $|v| \gg 1$. Then the properties (42) and (43) follow directly from (45), (46), (47) and (48). □

The orthonormality (37) implies that the mass matrix associated with the pair $(\tilde{\mathbb{T}}_N, \hat{\mathbb{T}}_N)$ is the identity matrix. Next, we consider the first order and second order stiffness matrices, denoted respectively by $\boldsymbol{S}^{(1)} = (s^{(1)}_{j,k})^N_{j,k=0}$ and $\boldsymbol{S}^{(2)} = (s^{(2)}_{j,k})^N_{j,k=0}$, with each entry defined by

$$s^{(1)}_{j,k} := \int_{\mathbb{R}} \left[v\tilde{T}_k(v)\right] \left[\frac{\partial}{\partial v}\hat{T}_j(v)\right] \mathrm{d}v, \tag{49}$$

$$s^{(2)}_{j,k} := \int_{\mathbb{R}} \left[\frac{\partial}{\partial v}\tilde{T}_k(v)\right] \left[\frac{\partial}{\partial v}\hat{T}_j(v)\right] \mathrm{d}v. \tag{50}$$

Recall the useful properties of Chebyshev polynomials: for $\forall k \geq 1$,

$$\xi T_k(\xi) = \frac{T_{k+1}(\xi) + T_{k-1}(\xi)}{2}, \tag{51}$$

$$(1-\xi^2)T_k'(\xi) = \frac{k}{2}\left(T_{k-1}(\xi) - T_{k+1}(\xi)\right). \tag{52}$$

Now we give the explicit formulas for the stiffness matrices in two useful cases: $r = 1$ for $\boldsymbol{S}^{(1)}$ and $r = 0$ for $\boldsymbol{S}^{(2)}$, based on the properties of Chebyshev polynomials shown above. These matrices will appear in the next subsection when we introduce the spectral method.

(I) The matrix $\boldsymbol{S}^{(1)}$ with $r = 1$. Starting from (49), we have

$$\begin{aligned} s^{(1)}_{j,k} &= \int_{-1}^{1} v(\xi)\mu^4(\xi)\frac{T_k(\xi)}{\sqrt{c_k}}\frac{\partial}{\partial\xi}\left(\mu^{-2}(\xi)\frac{T_j(\xi)}{\sqrt{c_j}}\right)\mathrm{d}\xi \\ &= \frac{1}{\sqrt{c_k c_j}}\int_{-1}^{1} v(\xi)T_k(\xi)\left(\mu^2 T_j'(\xi) - 2\mu\mu' T_j(\xi)\right)\mathrm{d}\xi. \end{aligned}$$

For $r=1$, $v(\xi)$ and $\mu(\xi)$ are given by (41). Then we have

$$s_{j,k}^{(1)}=\frac{1}{\sqrt{c_kc_j}}\left\{\int_{-1}^{1}\omega(\xi)\xi T_k(\xi)(1-\xi^2)T_j'(\xi)\mathrm{d}\xi+2\int_{-1}^{1}\omega(\xi)\xi^2T_k(\xi)T_j(\xi)\mathrm{d}\xi\right\}. \quad (53)$$

Using the properties (51)-(52), we have

$$\begin{aligned}
s_{j,k}^{(1,1)}&=\frac{1}{\sqrt{c_kc_j}}\int_{-1}^{1}\omega(\xi)\xi T_k(\xi)(1-\xi^2)T_j'(\xi)\mathrm{d}\xi\\
&=\frac{j}{4\sqrt{c_kc_j}}\int_{-1}^{1}\omega(\xi)\left[T_{k+1}(\xi)+T_{k-1}(\xi)\right]\left[T_{j-1}(\xi)-T_{j+1}(\xi)\right]\mathrm{d}\xi\\
&=\begin{cases}\frac{1}{\sqrt{2}}, & k=0,j=2,\\ \frac{1}{4}, & k=1,j=1,\\ \frac{j}{4}, & j=k+2,\ 1\le k\le N-2,\\ -\frac{j}{4}, & j=k-2,\ 3\le k\le N,\\ 0, & \text{otherwise;}\end{cases} \quad (54)\\
s_{j,k}^{(1,2)}&=\frac{1}{\sqrt{c_kc_j}}\int_{-1}^{1}\omega(\xi)\left[\xi T_k(\xi)\right]\left[\xi T_j(\xi)\right]\mathrm{d}\xi\\
&=\frac{1}{4\sqrt{c_kc_j}}\int_{-1}^{1}\omega(\xi)\left[T_{k+1}(\xi)+T_{k-1}(\xi)\right]\left[T_{j+1}(\xi)+T_{j-1}(\xi)\right]\mathrm{d}\xi\\
&=\begin{cases}\frac{1}{2}, & k=0,j=0,\\ \frac{3}{4}, & k=1,j=1,\\ \frac{1}{2\sqrt{2}}, & k=0,j=2 \text{ or } k=2,j=0,\\ \frac{1}{2}, & j=k\ge 2,\\ \frac{1}{4}, & j=k-2,\ 3\le k\le N \text{ or } j=k+2,\ 1\le k\le N-2,\\ 0, & \text{otherwise.}\end{cases} \quad (55)
\end{aligned}$$

It follows that for $r=1$, we have

$$s_{j,k}^{(1)}=s_{j,k}^{(1,1)}+2s_{j,k}^{(1,2)}. \quad (56)$$

(II) The matrix $\boldsymbol{S}^{(2)}$ with $r=0$. Starting from (50), we have

$$\begin{aligned}
s_{j,k}^{(2)}=&\frac{1}{\sqrt{c_kc_j}}\int_{-1}^{1}\frac{\partial}{\partial\xi}\left[\mu^4T_k(\xi)\right]\frac{\partial}{\partial\xi}\left[\mu^{-2}T_j(\xi)\right]\frac{\mathrm{d}\xi}{\mathrm{d}v}\mathrm{d}\xi\\
=&\frac{1}{\sqrt{c_kc_j}}\int_{-1}^{1}\left[4\mu^3\mu'T_k(\xi)+\mu^4T_k'(\xi)\right]\left[-2\mu^{-3}\mu'T_j(\xi)+\mu^{-2}T_j'(\xi)\right]\frac{\mu^2}{\omega}\mathrm{d}\xi\\
=&\frac{1}{S^2\sqrt{c_kc_j}}\left\{\int_{-1}^{1}\omega(1-\xi^2)^{r+2}T_k'(\xi)T_j'(\xi)\mathrm{d}\xi\right.\\
&-2(1+r)\int_{-1}^{1}\omega\xi(1-\xi^2)^{r+1}T_k(\xi)T_j'(\xi)\mathrm{d}\xi\\
&-(1+r)\int_{-1}^{1}\omega\xi(1-\xi^2)^{r+1}T_k'(\xi)T_j(\xi)\mathrm{d}\xi\\
&\left.+2(1+r)^2\int_{-1}^{1}\omega\xi^2(1-\xi^2)^rT_k(\xi)T_j(\xi)\mathrm{d}\xi\right\}. \quad (57)
\end{aligned}$$

For $r=0$, $\mu(\xi)$ is given by (40). Then we have

$$
\begin{aligned}
s_{j,k}^{(2,1)} :=& \frac{1}{S^2\sqrt{c_k c_j}} \int_{-1}^{1} \omega \left[(1-\xi^2)T_k'(\xi)\right] \left[(1-\xi^2)T_j'(\xi)\right] \mathrm{d}\xi \\
=& \begin{cases} \frac{3}{4S^2}, & k=1, j=1, \\ \frac{k^2}{2S^2}, & 2 \le k = j \le N, \\ -\frac{(k+2)(k+4)}{4S^2}, & j=k+2,\ 1 \le k \le N-2, \\ -\frac{k(k+2)}{4S^2}, & j=k-2,\ 3 \le k \le N, \\ 0, & \text{otherwise}; \end{cases}
\end{aligned} \tag{58}
$$

$$
\begin{aligned}
s_{j,k}^{(2,2)} :=& \frac{1}{S^2\sqrt{c_k c_j}} \int_{-1}^{1} \omega \left[\xi T_k(\xi)\right] \left[(1-\xi^2)T_j'(\xi)\right] \mathrm{d}\xi \\
=& \begin{cases} \frac{\sqrt{2}}{2S^2}, & k=0, j=2, \\ \frac{1}{2S^2}, & k=1, j=1, \\ \frac{k^2}{4S^2}, & 2 \le k = j \le N, \\ \frac{k+2}{4S^2}, & j=k+2,\ 1 \le k \le N-2, \\ -\frac{k-2}{4S^2}, & j=k-2,\ 3 \le k \le N, \\ 0, & \text{otherwise}; \end{cases}
\end{aligned} \tag{59}
$$

$$
\begin{aligned}
s_{j,k}^{(2,3)} :=& \frac{1}{S^2\sqrt{c_k c_j}} \int_{-1}^{1} \omega \left[\xi T_k(\xi)\right] \left[\xi T_j(\xi)\right] \mathrm{d}\xi \\
=& \frac{1}{S^2} s_{j,k}^{(1,2)},
\end{aligned} \tag{60}
$$

where $s_{j,k}^{(1,2)}$ is given in (55). It follows that for $r=0$, we have

$$
s_{jk}^{(2)} = s_{j,k}^{(2,1)} - 2s_{j,k}^{(2,2)} - s_{k,j}^{(2,2)} + 2s_{j,k}^{(2,3)}. \tag{61}
$$

3.2. **Petrov-Galerkin spectral methods for the inelastic Boltzmann equation.** We now introduce our spectral method for the inelastic Boltzmann equation using the previously defined mapped Chebyshev functions.

For the weak form (6), a Petrov-Galerkin method of the semi-discretization with respect to the variable v is: find $f_N(v,t) \in \tilde{\mathbb{V}}_N$ such that

$$
\frac{\partial}{\partial t}(f_N, \phi)_{\mathbb{R}} = \mathcal{Q}^{e,\lambda}(f_N, \phi), \quad \forall\, \phi \in \hat{\mathbb{V}}_N, \tag{62}
$$

where the operator $\mathcal{Q}^{e,\lambda}(\cdot,\cdot)$ is defined as

$$
\mathcal{Q}^{e,\lambda}(f,\phi) = \iint_{\mathbb{R}^2} B_\lambda(|v-w|) f(v) f(w) [\phi(v') - \phi(v)] \,\mathrm{d}v\,\mathrm{d}w, \tag{63}
$$

with v' given by

$$
v' = \frac{1}{2}(v+w) + \frac{e}{2}(v-w). \tag{64}
$$

The approximation function f_N is represented as the truncated mapped Chebyshev series

$$
f_N(v,t) = \sum_{k=0}^{N} \tilde{f}_k(t) \tilde{T}_k(v), \tag{65}
$$

where $\{\tilde{f}_k\}_{k=0}^N$ are the expansion coefficients depending on t and $\{\tilde{T}_k(v)\}_{k=0}^N$ are defined by (36). Let $\tilde{\mathbf{f}} = [\tilde{f}_0(t), \tilde{f}_1(t), \ldots, \tilde{f}_N(t)]^T$ denote the solution vector. Plugging

(65) to (62) yields the following system of ODEs

$$\frac{\mathrm{d}\tilde{\mathbf{f}}}{\mathrm{d}t} = \tilde{\boldsymbol{Q}}^{e,\lambda}(\tilde{\mathbf{f}}), \tag{66}$$

where $\tilde{\boldsymbol{Q}}^{e,\lambda}(\tilde{\mathbf{f}})$ is a vector with k-th component defined by

$$\begin{aligned}
\tilde{Q}_k^{e,\lambda} &= \int_{\mathbb{R}}\int_{\mathbb{R}} B_\lambda(|v-w|) f_N(v) f_N(w) \left[\hat{T}_k(v') - \hat{T}_k(v)\right] \mathrm{d}v\,\mathrm{d}w \\
&= \sum_{i,j} \tilde{f}_i \tilde{f}_j \int_{\mathbb{R}}\int_{\mathbb{R}} B_\lambda(|v-w|) \tilde{T}_i(v)\tilde{T}_j(w) \left[\hat{T}_k(v') - \hat{T}_k(v)\right] \mathrm{d}v\,\mathrm{d}w \\
&:= \sum_{i,j} \tilde{f}_i \tilde{f}_j \left[\tilde{I}_1(i,j,k) - \tilde{I}_2(i,j,k)\right],
\end{aligned} \tag{67}$$

where the integrals $\tilde{I}_1(i,j,k)$ and $\tilde{I}_2(i,j,k)$ are given, respectively, as follows:

$$\begin{aligned}
\tilde{I}_1(i,j,k) &= \int_{\mathbb{R}}\int_{\mathbb{R}} B_\lambda(|v-w|)\tilde{T}_i(v)\tilde{T}_j(w)\hat{T}_k(v')\,\mathrm{d}v\,\mathrm{d}w \\
&= \int_{-1}^{1}\int_{-1}^{1} B_\lambda(|v-w|) \frac{[\mu(\xi(v))]^4}{\sqrt{c_i}} T_i(\xi(v)) \frac{[\mu(\xi(w))]^4}{\sqrt{c_j}} T_j(\xi(w)) \frac{T_k(\xi(v'))}{[\mu(\xi(v'))]^2\sqrt{c_k}} \\
&\quad \cdot \frac{\mathrm{d}v}{\mathrm{d}\xi(v)} \frac{\mathrm{d}w}{\mathrm{d}\xi(w)} \mathrm{d}\xi(v)\mathrm{d}\xi(w) \\
&= \int_{-1}^{1}\int_{-1}^{1} \omega(\xi(v))\omega(\xi(w)) \frac{T_i(\xi(v))T_j(\xi(w))}{\sqrt{c_i c_j}} \frac{B_\lambda(|v-w|)T_k(\xi(v'))}{\sqrt{c_k}} \\
&\quad \cdot \left[\frac{\mu(\xi(v))\mu(\xi(w))}{\mu(\xi(v'))}\right]^2 \mathrm{d}\xi(v)\mathrm{d}\xi(w),
\end{aligned} \tag{68}$$

$$\begin{aligned}
\tilde{I}_2(i,j,k) &= \int_{\mathbb{R}}\int_{\mathbb{R}} B_\lambda(|v-w|)\tilde{T}_i(v)\tilde{T}_j(w)\hat{T}_k(v)\,\mathrm{d}v\,\mathrm{d}w, \\
&= \int_{-1}^{1}\int_{-1}^{1} \omega(\xi(v))\omega(\xi(w)) \frac{T_i(\xi(v))T_j(\xi(w))}{\sqrt{c_i c_j}} \frac{B_\lambda(|v-w|)T_k(\xi(v))[\mu(\xi(w))]^2}{\sqrt{c_k}} \\
&\quad \cdot \mathrm{d}\xi(v)\mathrm{d}\xi(w).
\end{aligned} \tag{69}$$

Therefore, for each fixed k, $\tilde{I}_1(i,j,k)$ and $\tilde{I}_2(i,j,k)$ are the forward Chebyshev transforms of the 2D functions $\frac{B_\lambda(|v-w|)T_k(\xi(v'))}{\sqrt{c_k}}\left[\frac{\mu(\xi(v))\mu(\xi(w))}{\mu(\xi(v'))}\right]^2$ and $\frac{B_\lambda(|v-w|)T_k(\xi(v))[\mu(\xi(w))]^2}{\sqrt{c_k}}$, respectively, which can be computed efficiently using the fast Chebyshev transform.

I. With the **velocity rescaling**, one should use the weak form (17), whose Petrov-Galerkin approximation is: find $g_N(v,t) = \sum_{k=0}^{N} \tilde{g}_k(t)\tilde{T}_k(v) \in \hat{\mathbb{V}}_N$ such that

$$\frac{\partial}{\partial t}(g_N, \phi)_{\mathbb{R}} = \frac{1-e^2}{4}\mathcal{S}^{(1)}(g_N,\phi) + \mathcal{Q}^{e,0}(g_N,\phi), \quad \forall\, \phi \in \hat{\mathbb{V}}_N, \tag{70}$$

where the operators $\mathcal{Q}^{e,0}$ is the special case of (63) when $\lambda = 0$ and $\mathcal{S}^{(1)}(\cdot,\cdot)$ is defined as

$$\mathcal{S}^{(1)}(g,\phi) = \int vg\frac{\partial \phi}{\partial v}\,\mathrm{d}v. \tag{71}$$

Using the same vector notation as before, (70) becomes

$$\frac{\mathrm{d}\tilde{\mathbf{g}}}{\mathrm{d}t} = \frac{1-e^2}{4}\boldsymbol{S}^{(1)}\tilde{\mathbf{g}} + \tilde{\boldsymbol{Q}}^{e,0}(\tilde{\mathbf{g}}), \tag{72}$$

where the matrix $\boldsymbol{S}^{(1)}$ is defined in (49), and $\tilde{\boldsymbol{Q}}^{e,0}$ is the special case of $\tilde{\boldsymbol{Q}}^{e,\lambda}$ when $\lambda = 0$.

II. With the **heated term**, one starts with the weak form (21), whose Petrov-Galerkin approximation is: find $f_N(v,t) \in \tilde{\mathbb{V}}_N$ such that

$$\frac{\partial}{\partial t}(f_N, \phi)_{\mathbb{R}} = \mathcal{Q}^{e,\lambda}(f_N, \phi) - \varepsilon \mathcal{S}^{(2)}(f_N, \phi), \quad \forall\, \phi \in \hat{\mathbb{V}}_N, \tag{73}$$

where the operator $\mathcal{S}^{(2)}(\cdot,\cdot)$ is defined as

$$\mathcal{S}^{(2)}(f, \phi) = \int_{\mathbb{R}} \frac{\partial f}{\partial v}\frac{\partial \phi}{\partial v}\,\mathrm{d}v. \tag{74}$$

Using the same vector notation as before, (73) becomes

$$\frac{\mathrm{d}\tilde{\mathbf{f}}}{\mathrm{d}t} = \tilde{\boldsymbol{Q}}^{e,\lambda}(\tilde{\mathbf{f}}) - \varepsilon \boldsymbol{S}^{(2)}\tilde{\mathbf{f}}, \tag{75}$$

where the matrix $\boldsymbol{S}^{(2)}$ is defined in (50).

Remark 1. The time discretization for the ODE systems (66), (72) and (75) is immaterial since there is no stiff term in these equations. The numerical results presented in the next section are obtained using a fourth order explicit Runge-Kutta scheme.

Remark 2. In the case of velocity rescaling, if the particles are non-Maxwell molecules, one needs to solve an additional equation for $T(t)$. This can be done in the same spectral framework proposed here. We omit the detail.

3.3. **Approximation property for the function.** Now we consider the error estimates for mapped Chebyshev approximations. Without loss of generality, we assume the scaling parameter $S = 1$ in the μ defined by (30).

Let $\mathbb{P}_N$ be the set of polynomials with degree less than or equal to N and define a more general approximation space with a parameter α,

$$\mathbb{V}_N^\alpha := \operatorname{span}\left\{T_k^\alpha(v) := [\mu(\xi(v))]^\alpha T_k(\xi(v)),\ k = 0, 1, \ldots, N\right\}. \tag{76}$$

Our two sets of approximation spaces correspond to $\alpha = 4$ and $\alpha = -2$, respectively, i.e.,

$$\tilde{\mathbb{V}}_N = \mathbb{V}_N^4 = \operatorname{span}\left(\tilde{\mathbb{T}}_N\right), \quad \hat{\mathbb{V}}_N = \mathbb{V}_N^{-2} = \operatorname{span}\left(\hat{\mathbb{T}}_N\right). \tag{77}$$

In what follows, in addition to the pair (u, U) shown in (31), we use $(\hat{u}^\alpha, \widehat{U}^\alpha)$ to denote another pair related by:

$$\hat{u}^\alpha(v) = u(v)[\mu(\xi(v))]^{-\alpha} = U(\xi(v))[\mu(\xi(v))]^{-\alpha} = \widehat{U}^\alpha(\xi(v)). \tag{78}$$

Let $\omega(\xi)$ be the Chebyshev weight defined by (28) and $\Pi_N^c : L^2_\omega(I) \to \mathbb{P}_N$ be the Chebyshev orthogonal projection defined by

$$\left(\Pi_N^c U - U, \Phi\right)_{L^2_\omega(I)} = 0, \quad \forall \Phi \in \mathbb{P}_N. \tag{79}$$

Let $\mu(\xi(v))$ be defined in (30). We define the projector $\pi_N^\alpha u : L^2_{\mu^{2-2\alpha}}(\mathbb{R}) \to \mathbb{V}_N^\alpha$ by

$$\pi_N^\alpha u := \mu^\alpha \Pi_N^c(U\mu^{-\alpha}) = \mu^\alpha(\Pi_N^c \widehat{U}^\alpha) \in \mathbb{V}_N^\alpha. \tag{80}$$

We verify from the definition that

$$\begin{aligned}\int_{-\infty}^{\infty}(\pi_N^\alpha u-u)T_k^\alpha(v)\,\mu^{2-2\alpha}\,\mathrm{d}v &= \int_{-1}^{1}\big(\Pi_N^c(U\mu^{-\alpha})-(U\mu^{-\alpha})\big)T_k(\xi)\mu^2\frac{\mathrm{d}v}{\mathrm{d}\xi}\mathrm{d}\xi\\ &= \int_{-1}^{1}\big(\Pi_N^c\widehat{U}^\alpha-\widehat{U}^\alpha\big)T_k(\xi)\omega(\xi)\mathrm{d}\xi=0,\quad \forall 0\le k\le N.\end{aligned}\tag{81}$$

To describe the approximation error, we introduce the following differential operator:

$$D_{\alpha,v}u := a(v)\frac{\mathrm{d}}{\mathrm{d}v}\hat{u}^\alpha,\tag{82}$$

where $a(v)=\frac{\mathrm{d}v}{\mathrm{d}\xi}$ is defined by (29) and $\hat{u}^\alpha(v)=u(v)[\mu(\xi(v))]^{-\alpha}$.

We can derive by recursion that

$$\begin{aligned}\frac{\mathrm{d}\widehat{U}^\alpha}{\mathrm{d}\xi} &= a\frac{\mathrm{d}\hat{u}^\alpha}{\mathrm{d}v} := D_{\alpha,v}u,\\ \frac{\mathrm{d}^2\widehat{U}^\alpha}{\mathrm{d}\xi^2} &= a\frac{\mathrm{d}}{\mathrm{d}v}\Big(a\frac{\mathrm{d}\hat{u}^\alpha}{\mathrm{d}v}\Big) := D_{\alpha,v}^2u,\\ &\vdots\\ \frac{\mathrm{d}^k\widehat{U}^\alpha}{\mathrm{d}\xi^k} &= a\frac{\mathrm{d}}{\mathrm{d}v}\underbrace{\Big(a\frac{\mathrm{d}}{\mathrm{d}v}\Big(\cdots\cdots\Big(a\frac{\mathrm{d}\hat{u}^\alpha}{\mathrm{d}v}\Big)\cdots\Big)\Big)}_{k-1\ \text{parentheses}} := D_{\alpha,v}^ku.\end{aligned}\tag{83}$$

Next, we define the following function space

$$B_\alpha^m(\mathbb{R})=\big\{u:\ u\ \text{ is measurable in } \mathbb{R} \text{ and } \|u\|_{B_\alpha^m(\mathbb{R})}<\infty\big\},\tag{84}$$

equipped with the norm and semi-norm

$$\|u\|_{B_\alpha^m(\mathbb{R})}=\Big(\sum_{k=0}^{m}\big\|D_{\alpha,v}^ku\big\|^2_{L^2_{\varpi^{k+(1+r)/2}}(\mathbb{R})}\Big)^{1/2},\quad |u|_{B^m(\mathbb{R})}=\big\|D_{\alpha,v}^mu\big\|_{L^2_{\varpi^{m+(1+r)/2}}(\mathbb{R})}\tag{85}$$

where the weight function $\varpi^s(v):=(1-\xi^2(v))^s$.

We are now ready to present the main results on the mapped Chebyshev approximations.

Theorem 3.2. *Consider $\alpha\in\mathbb{R}$, $r\ge 0$. If $u\in B_\alpha^m(\mathbb{R})$, we have*

$$\big\|\pi_N^\alpha u-u\big\|_{L^2_{\mu^{2-2\alpha}}(\mathbb{R})}\lesssim N^{-m}\big\|D_{\alpha,v}^mu\big\|_{L^2_{\varpi^{m+(1+r)/2}}(\mathbb{R})}.\tag{86}$$

Proof. We recall [37] that

$$\big\|\Pi_N^cU-U\big\|_{L^2_\omega(I)}\lesssim N^{-m}\|d_\xi^mU\|_{L^2_{(1-\xi^2)^{m-1/2}}(I)}.$$

On the other hand, similar to (81), we have

$$\begin{aligned}\int_{-\infty}^{\infty}(\pi_N^\alpha u-u)^2\,\mu^{2-2\alpha}\,\mathrm{d}v &= \int_{-1}^{1}\big(\Pi_N^c(U\mu^{-\alpha})-(U\mu^{-\alpha})\big)^2\mu^2\frac{\mathrm{d}v}{\mathrm{d}\xi}\mathrm{d}\xi\\ &= \int_{-1}^{1}\big(\Pi_N^c\widehat{U}^\alpha-\widehat{U}^\alpha\big)^2\omega(\xi)\,\mathrm{d}\xi.\end{aligned}\tag{87}$$

Hence

$$\begin{aligned}\left\|\pi_N^\alpha u - u\right\|_{L^2_{\mu^{2-2\alpha}}(\mathbb{R})} &= \left\|\Pi_N^c \widehat{U}^\alpha - \widehat{U}^\alpha\right\|_{L^2_\omega(I)} \\ &\lesssim N^{-m}\|d_\xi^m \widehat{U}^\alpha\|_{L^2_{(1-\xi^2)^{m-1/2}}(I)} \lesssim N^{-m}\left\|D^m_{\alpha,v}u\right\|_{L^2_{\varpi^{m+(1+r)/2}}(\mathbb{R})}.\end{aligned} \tag{88}$$

□

3.4. **Approximation property for the moments.** We show below that our Petrov-Galerkin method enjoys excellent approximation properties for physically important moments such as mass, momentum and energy.

Theorem 3.3. *In the velocity rescaling case ($r = 1$), the functions 1 and v^2 are included in the test space $\hat{\mathbb{V}}_N$ so that the mass and energy are automatically conserved; on the other hand, the error estimate for the momentum is given by*

$$|(g, v)_\mathbb{R} - (g, \pi_N^{-2} v)_\mathbb{R}| \lesssim \|g\|_{L^2_{\mu^{-6}}(\mathbb{R})} N^{-2}. \tag{89}$$

Furthermore, the convergence rate can be improved for smoother g:

$$|(g, v)_\mathbb{R} - (g, \pi_N^{-2} v)_\mathbb{R}| \lesssim \|D^m_{-2,v}(g\mu^{-6})\|_{L^2_{\varpi^{m+1}}(\mathbb{R})} N^{-2-m}. \tag{90}$$

In the heated case ($r = 0$), the error estimate for any moment v^k ($k = 0, 1, 2, \ldots$ integer) is given by

$$|(f, v^k)_\mathbb{R} - (f, \pi_N^{-2} v^k)_\mathbb{R}| \lesssim \|f\|_{L^2_{\mu^{-6}}(\mathbb{R})} N^{-1}. \tag{91}$$

Furthermore, the convergence rate can be improved for smoother f:

$$|(f, v^k)_\mathbb{R} - (f, \pi_N^{-2} v^k)_\mathbb{R}| \lesssim \|D^m_{-2,v}(f\mu^{-6})\|_{L^2_{\varpi^{m+1/2}}(\mathbb{R})} N^{-1-m}. \tag{92}$$

Proof. We recall that in the case of velocity rescaling, we use the algebraic mapping (41), while in the heated case we use the logarithmic mapping (40). **The velocity rescaling case.** We show first that with $r = 1$, the functions 1 and v^2 are included in the test space $\hat{\mathbb{V}}_N$ so that the zeroth and second moments are automatically conserved. Starting from the first three Chebyshev polynomials

$$T_0(\xi) = 1, \quad T_1(\xi) = \xi, \quad T_2(\xi) = 2\xi^2 - 1, \tag{93}$$

we can get

$$T_0(\xi(v)) = 1, \quad T_1(\xi(v)) = \frac{v}{\sqrt{S^2 + v^2}}, \quad T_2(\xi(v)) = \frac{v^2 - S^2}{v^2 + S^2}, \tag{94}$$

$$\Longrightarrow \hat{T}_0(\xi(v)) = \frac{v^2 + S^2}{S}, \quad \hat{T}_1(\xi(v)) = \frac{v}{S}\sqrt{v^2 + S^2}, \quad \hat{T}_2(\xi(v)) = \frac{v^2 - S^2}{S}, \tag{95}$$

$$\Longrightarrow 1 = \frac{1}{2S}\left(\hat{T}_0(\xi(v)) - \hat{T}_2(\xi(v))\right), \quad v^2 = \frac{S}{2}\left(\hat{T}_0(\xi(v)) + \hat{T}_2(\xi(v))\right), \tag{96}$$

which show that 1 and v^2 are included in the test space $\hat{\mathbb{V}}_N = \mathbb{V}_N^{-2}$. Unfortunately, v is not in the test space. But we can easily check that

$$\left\|D^m_{\alpha,v} v\right\|_{L^2_{\varpi^{m+1}}(\mathbb{R})} < \infty \quad \text{for} \;\; m = 0, 1, 2 \;\; \text{and} \;\; \alpha = -2. \tag{97}$$

Thanks to Theorem 3.2, we can derive from (86) with $\alpha = -2, m = 2$ that

$$\|v - \pi_N^{-2} v\|_{L^2_{\mu^6}(\mathbb{R})} \lesssim N^{-2}. \tag{98}$$

Hence, the first moment $(g,v)_{\mathbb{R}}$ can be approximated by our Petrov-Galerkin method $(g,\pi_N^{-2}v)_{\mathbb{R}}$ with error

$$|(g,v)_{\mathbb{R}}-(g,\pi_N^{-2}v)_{\mathbb{R}}|\le\|g\|_{L^2_{\mu^{-6}}(\mathbb{R})}\|v-\pi_N^{-2}v\|_{L^2_{\mu^6}(\mathbb{R})}\lesssim\|g\|_{L^2_{\mu^{-6}}(\mathbb{R})}N^{-2}. \tag{99}$$

Furthermore, the convergence rate can be improved for smoother g. Indeed, we recall from (81) that

$$(v-\pi_N^{-2}v,w_N)_{\mu^6}=0\quad\forall w_N\in\mathbb{V}_N^{-2}. \tag{100}$$

Hence, we derive from the above, (98) and (86) that

$$\begin{aligned}&|(g,v)_{\mathbb{R}}-(g,\pi_N^{-2}v)_{\mathbb{R}}|\\&\quad=|(g,v-\pi_N^{-2}v)_{\mathbb{R}}|=|(g\mu^{-6},v-\pi_N^{-2}v)_{\mu^6}|\\&\quad=|(g\mu^{-6}-\pi_N^{-2}(g\mu^{-6}),v-\pi_N^{-2}v)_{\mu^6}|\lesssim\|g\mu^{-6}-\pi_N^{-2}(g\mu^{-6})\|_{\mu^6}N^{-2}\\&\quad\lesssim\|D^m_{-2,v}(g\mu^{-6})\|_{L^2_{\varpi^{m+1}}(\mathbb{R})}N^{-2-m}.\end{aligned} \tag{101}$$

The heated case. In this case $r=0$, and the polynomials $\{1,v,v^2\}$ are not in the test space $\hat{\mathbb{V}}_N$. However, we shall show below $\left\|D^m_{\alpha,v}(v^k)\right\|_{L^2_{\varpi^{m+1/2}}(\mathbb{R})}<\infty$ for $\alpha=-2$, $m=0,1$, and any integer $k=0,1,2,\ldots$. For the sake of notational simplicity, let us assume $S=1$. We have

$$[\mu(\xi(v))]^2=(1-\xi^2)^{1/2}=\frac{2}{\mathrm{e}^{v/S}+\mathrm{e}^{-v}}=\operatorname{sech}(v)\,, \tag{102}$$

$$a(v)=\frac{\mathrm{d}v}{\mathrm{d}\xi}=(1-\xi^2)^{-1}=\left(\frac{\mathrm{e}^v+\mathrm{e}^{-v}}{2}\right)^2=\cosh^2(v), \tag{103}$$

$$\varpi^{m+1/2}(v)=(1-\xi^2)^{m+1/2}=\left(\frac{2}{\mathrm{e}^v+\mathrm{e}^{-v}}\right)^{2m+1}=\operatorname{sech}^{2m+1}(v)\,. \tag{104}$$

It follows that for $m=0$, we have

$$\|D^0_{\alpha,v}(v^k)\|^2_{L^2_{\varpi^{1/2}}(\mathbb{R})}=\int_{\mathbb{R}}v^{2k}\operatorname{sech}^3(v)\,\mathrm{d}v<\infty. \tag{105}$$

For $m=1$, we have

$$\|D^1_{\alpha,v}(v^k)\|^2_{L^2_{\varpi^{3/2}}(\mathbb{R})}=\int_{\mathbb{R}}\frac{1}{\operatorname{sech}(v)}\left[\frac{\mathrm{d}}{\mathrm{d}v}\left(v^k\operatorname{sech}(v)\right)\right]^2\mathrm{d}v \tag{106}$$

$$=\int_{\mathbb{R}}\left(v^{2k}\tanh^2(v)\operatorname{sech}(v)+\text{terms with faster decay}\right)\mathrm{d}v \tag{107}$$

$$<\infty. \tag{108}$$

It follows from (86) with $\alpha=-2,m=1$ in Theorem 3.2 that

$$\|v^k-\pi_N^{-2}v^k\|_{L^2_{\mu^6}(\mathbb{R})}\lesssim N^{-1}. \tag{109}$$

Then

$$|(f,v^k)_{\mathbb{R}}-(f,\pi_N^{-2}v^k)_{\mathbb{R}}|\le\|f\|_{L^2_{\mu^{-6}}(\mathbb{R})}\|v^k-\pi_N^{-2}v^k\|_{L^2_{\mu^6}(\mathbb{R})}\lesssim\|f\|_{L^2_{\mu^{-6}}(\mathbb{R})}N^{-1}. \tag{110}$$

Furthermore, with smoother f, one can derive similarly as above that

$$|(f,v^k)_{\mathbb{R}}-(f,\pi_N^{-2}v^k)_{\mathbb{R}}|\lesssim\|D^m_{-2,v}(f\mu^{-6})\|_{L^2_{\varpi^{m+1/2}}(\mathbb{R})}N^{-1-m}. \tag{111}$$

□

Remark 3. We recall that in the Fourier Galerkin method [34, 16], only the zeroth moment is preserved, while the first and second moments converge as $N^{-1/2}$ and $N^{-3/2}$ (for $f \in L^2$), respectively. For our method, (i) in the velocity rescaling case ($r = 1$), the method preserves exactly the zeroth and second moments, and the first moment converges as N^{-2} (for $g \in L^2_{\mu^{-6}}$), and (ii) in the heated case ($r = 0$), all polynomial moments converge as N^{-1} (for $f \in L^2_{\mu^{-6}}$). Hence, our Petrov-Galerkin methods improve over the Fourier Galerkin method with respect to physically important moments (for $r = 1$ the rate is better for first three moments; for $r = 0$ all polynomial moments decay). If the function f is smooth, then all methods would converge exponentially.

Furthermore, the test and trial functions in our Petrov-Galerkin methods enjoy the following nice properties:

- They are orthogonal to each other which leads to the sparsity in the mass and stiffness matrices.
- They are linked to the Chebyshev polynomials so that fast transforms between function values and expansion coefficients are available through FFT.

4. Numerical examples.

In this section, we present several numerical examples showing the accuracy of the proposed spectral method. We first compare the approximation errors obtained from Fourier and mapped Chebyshev approximations for the typical steady state functions appearing in the inelastic Boltzmann equation. Then we use the method to solve the equation.

4.1. Approximation results.

First, let us consider the spectral approximation to the functions $\{M_k(v)\}_{k=0}^3$ defined in (18), (19), (25) and (26), whose plots are shown in Figure 1.

We compare the results from three methods:

(1) **Fourier**: Fourier approximation in truncated domain $[-L, L]$;
(2) **Chebyshev-0**: Mapped Chebyshev approximation with $r = 0$;
(3) **Chebyshev-1**: Mapped Chebyshev approximation with $r = 1$.

We choose $L = 16$ in Fourier approximation and the scaling parameter $S = 4$ in mapped Chebyshev approximations. The numerical results are shown in Figures 2 - 3, where the L^2 error is defined as $\left(\int_{-L}^{L}(M_{\text{ext}}(v) - M_{\text{num}}(v))^2 \mathrm{d}v\right)^{1/2}$ in the Fourier method and $\left(\int_{\mathbb{R}}(M_{\text{ext}}(v) - M_{\text{num}}(v))^2 \mathrm{d}v\right)^{1/2}$ in the Chebyshev method. We can observe that:

- For the functions $M_0(v), M_2(v)$ and $M_3(v)$, the tails of which decay exponentially, the mapped Chebyshev approximation with both $r = 0$ and $r = 1$ perform better than Fourier approximation.
- For the function $M_1(v)$ with algebraic decay, the mapped Chebyshev approximation with $r = 0$ does not converge. However, the mapped Chebyshev approximation with $r = 1$ performs much better than Fourier approximation. In fact, this is the reason we use $r = 1$ in the rescaled case and $r = 0$ in the heated case when solving the equations later.

4.2. Solving the inelastic Boltzmann equation.

We now test the spectral methods described in Section 3.2 for solving the inelastic Boltzmann equation. The fourth order explicit Runge-Kutta scheme is used for time discretization. For

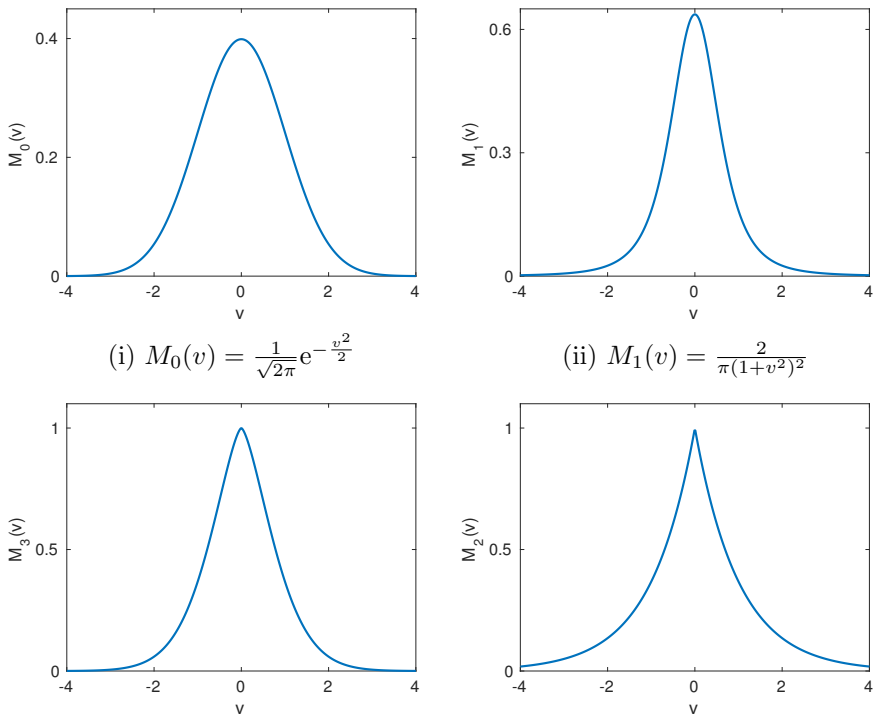

(i) $M_0(v) = \frac{1}{\sqrt{2\pi}} \mathrm{e}^{-\frac{v^2}{2}}$ (ii) $M_1(v) = \frac{2}{\pi(1+v^2)^2}$

(iii) $M_2(v) = \mathrm{e}^{-|v|}$ (iv) $M_3(v) = \mathrm{e}^{-|v|^{3/2}}$

FIGURE 1. Functions to be approximated.

simplicity, we will restrict to Maxwell molecules and consider the following initial condition

$$f(v,0) = \frac{1}{\sqrt{2\pi}} \exp\left(-\frac{v^2}{2}\right). \tag{112}$$

4.2.1. *Classical variables.* Let us first solve the inelastic Boltzmann equation written in the original variable, i.e., the problem (62).

In the numerical test, we use the method **Chebyshev-0** with $N = 256, S = 8$ in velocity discretization, the time step is chosen as $\Delta t = 0.005$, and the restitution coefficient $e = 0.25$. The numerical solutions of f at time $t = 5, 10, 15, 20$ are shown in Figure 4, which verifies that the solution formally converges to the Dirac delta function. Furthermore, the numerical zero, first, and second order moments of f and their errors are shown in Figure 5. We observe spurious oscillations due to the Gibbs phenomenon and thus we have a marked deterioration of accuracy in the moments.

As discussed earlier, there are two different strategies that may serve as a remedy to this problem: (1) velocity rescaling and (2) adding a diffusion term.

4.2.2. *Rescaled variables.* We now solve the problem (70) using the method **Chebyshev-1** with $N = 256, S = 8$ in velocity discretization. The numerical solutions of g for $e = 0.25$ in rescaled variables at time $t = 5, 10, 15, 20$ are shown in part (i) and (ii) in Figure 6. Using the relation (11), we can transform back to

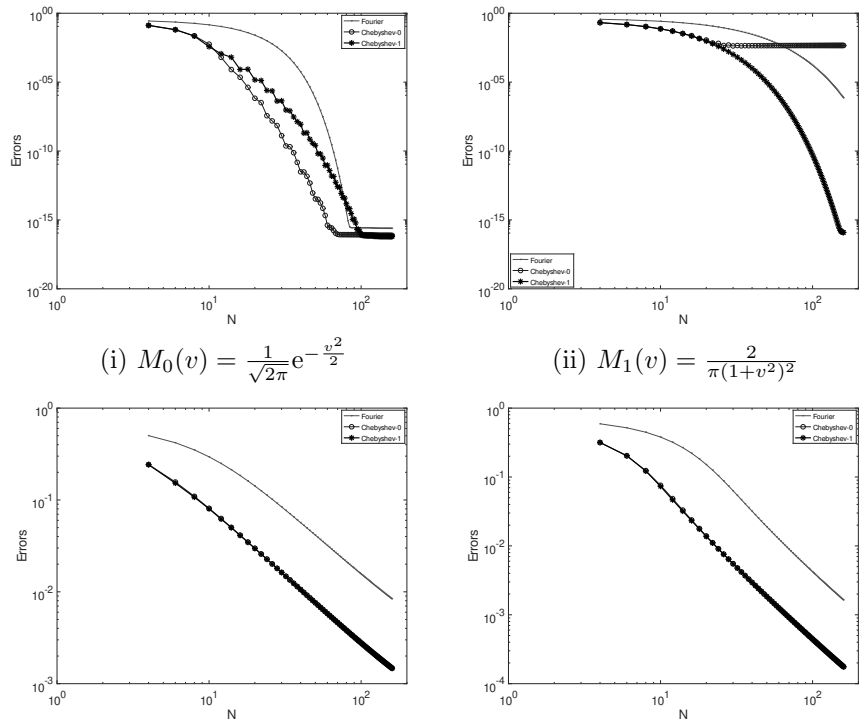

(i) $M_0(v) = \frac{1}{\sqrt{2\pi}} \mathrm{e}^{-\frac{v^2}{2}}$ (ii) $M_1(v) = \frac{2}{\pi(1+v^2)^2}$

(iii) $M_2(v) = \mathrm{e}^{-|v|}$ (iv) $M_3(v) = \mathrm{e}^{-|v|^{3/2}}$

FIGURE 2. L_2 errors in log-log scale.

the original function f, which are shown in part (iii) and (iv) in Figure 6. We can observe that the solutions are captured well without oscillations after rescaling.

Furthermore, we consider the case $e = 0.75$. The numerical results are shown in Figures 7. Also, the errors of the zeroth and second numerical moments of g are shown in Figure 8 (the result of the first moment is omitted as it can be captured well due to the symmetry of the solution), which verify our claims in Section 3.4 that the zeroth and second moments are conserved up to the time discretization error.

4.2.3. *Heated case.* For the heated problem (73) with $\lambda = 0$, we use the method **Chebyshev-0** with $N = 256, S = 8$ in velocity discretization. We consider the cases with $\varepsilon = 0.1, 0.01$ and $e = 0.25, 0.75$. The numerical solutions at time $t = 20$ are shown in Figure 9. The numerical moments for $\varepsilon = 0.01$ as well as the errors are shown in Figures 10 and 12.

Also, the errors of moments with respect to different N are shown in Figure 11 and Figure 13.

5. **Concluding remarks.** We introduced a Petrov-Galerkin spectral method for solving the inelastic Boltzmann equation. Solutions to such equations usually exhibit heavy tails in the velocity space which requires large computational domain. Our method is based on the mapped Chebyshev functions on unbounded domains so that domain truncation is not required. Furthermore, instead of the usual Galerkin

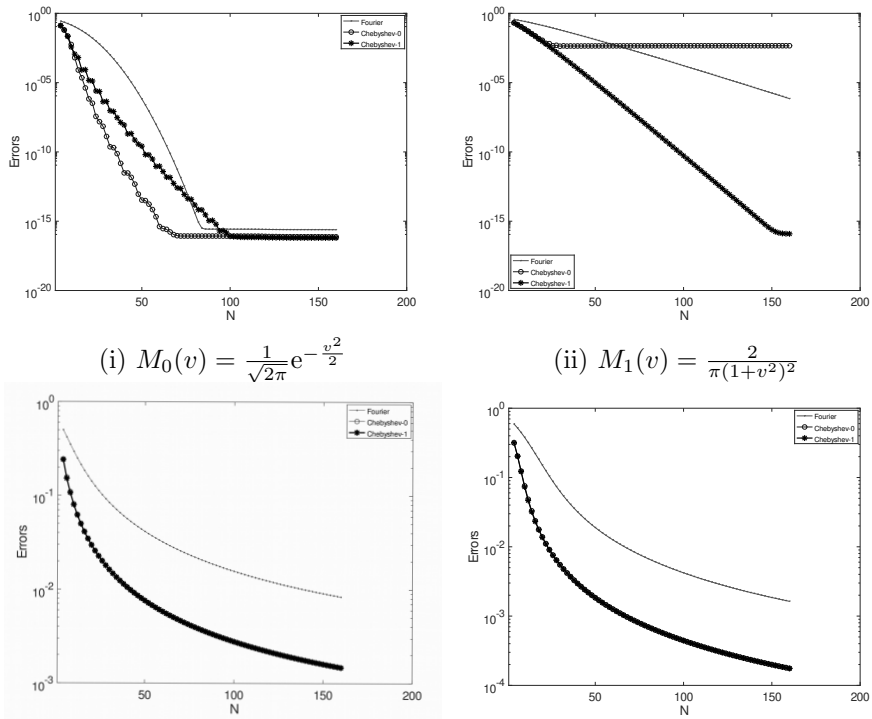

(i) $M_0(v) = \frac{1}{\sqrt{2\pi}} \mathrm{e}^{-\frac{v^2}{2}}$ (ii) $M_1(v) = \frac{2}{\pi(1+v^2)^2}$

(iii) $M_2(v) = \mathrm{e}^{-|v|}$ (iv) $M_3(v) = \mathrm{e}^{-|v|^{3/2}}$

FIGURE 3. L_2 errors in linear-log scale.

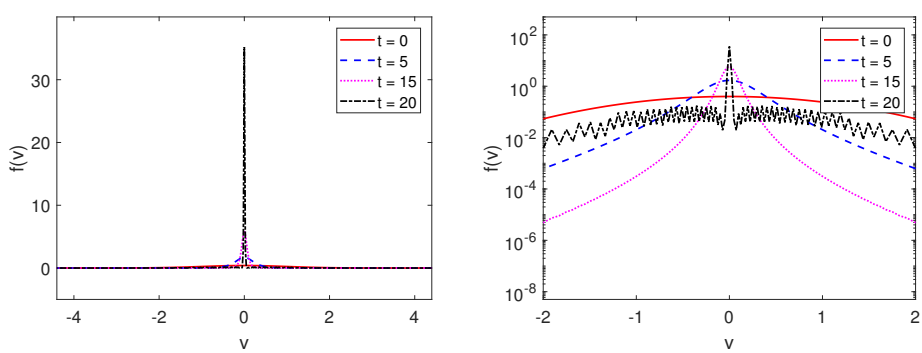

(i) overall (ii) zoomed (log scale)

FIGURE 4. Numerical solutions of f at time $t = 0, 5, 10, 20$ with $e = 0.25$.

approach, we devised a Petrov-Galerkin approach with carefully chosen trial and test spaces such that (i) in the rescaled case with $r = 1$, it conserves the mass and energy exactly and provides very good approximation of the momentum; (ii) in the heated case, all the three moments converge exponentially.

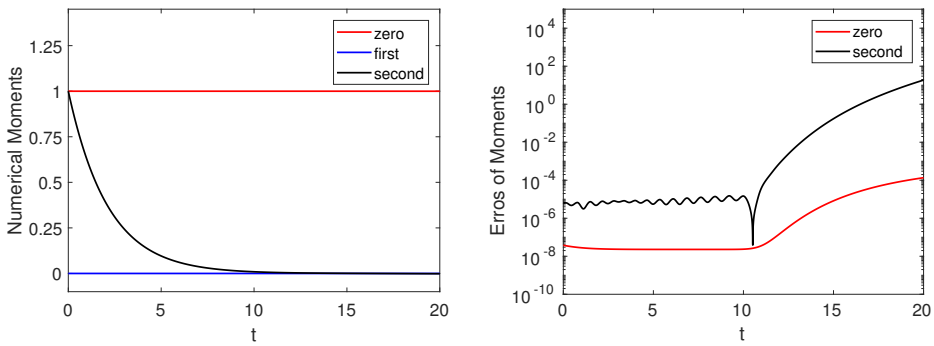

(i) moments (ii) errors

FIGURE 5. Numerical moments of f from $t = 0$ to $t = 20$ with $e = 0.25$.

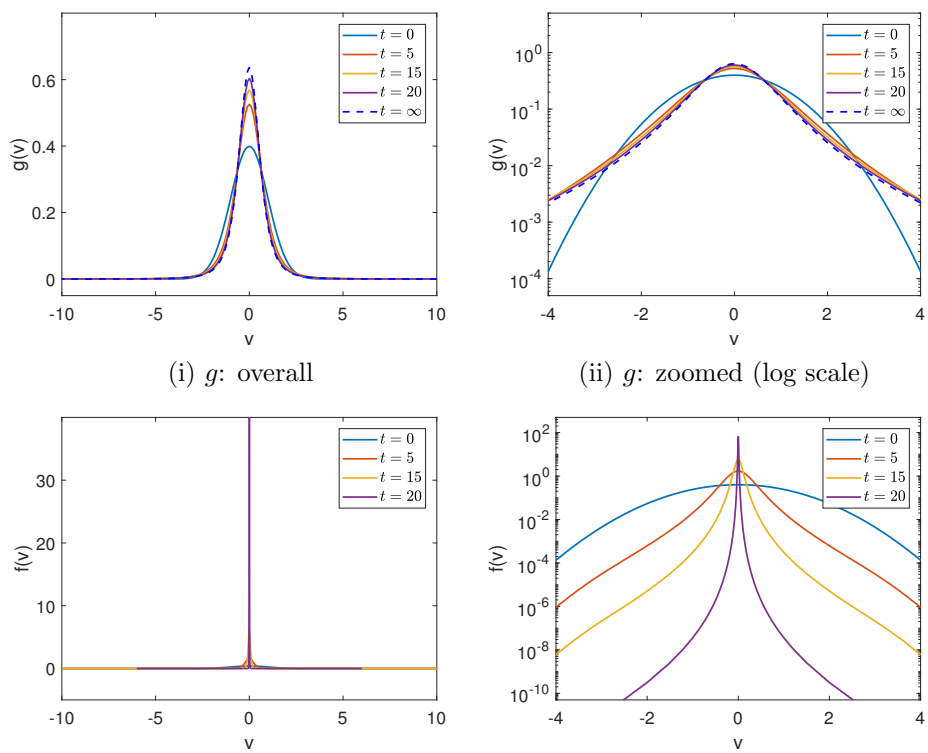

(i) g: overall (ii) g: zoomed (log scale)

(iii) back to f: overall (iv) back to f: zoomed (log scale)

FIGURE 6. Numerical solutions in the rescaled case at time $t = 0, 5, 10, 20$ with $e = 0.25$.

Through a series of examples, we showed that the proposed method performs much better than the Fourier spectral method and yields accurate results. This

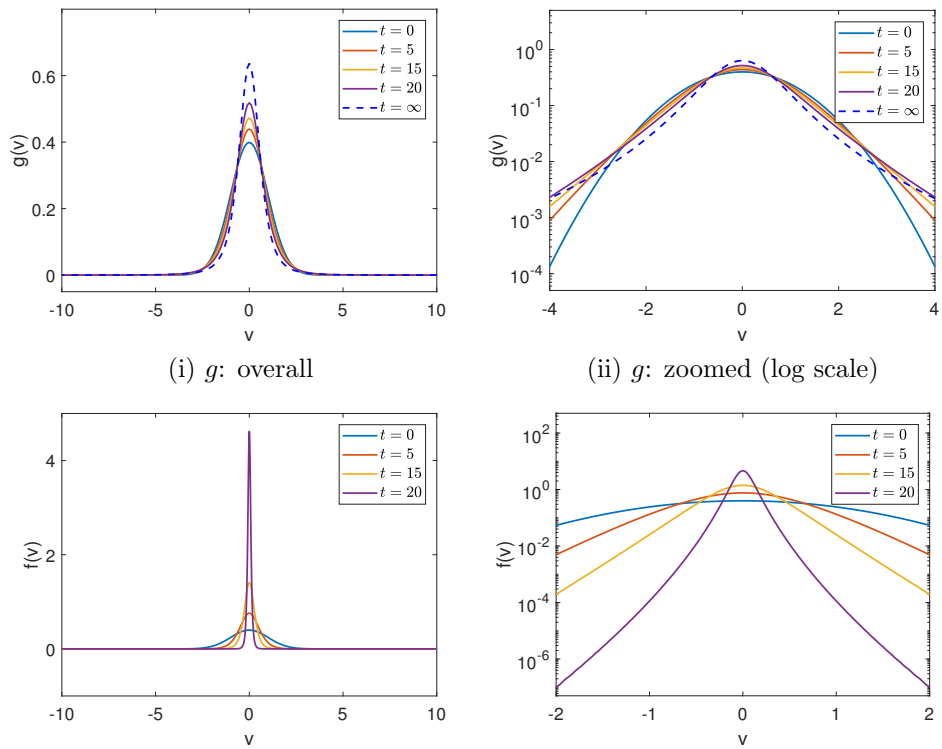

(i) g: overall (ii) g: zoomed (log scale)

(iii) back to f: overall (iv) back to f: zoomed (log scale)

FIGURE 7. Numerical solutions in the rescaled case at time $t = 0, 5, 10, 20$ with $e = 0.75$.

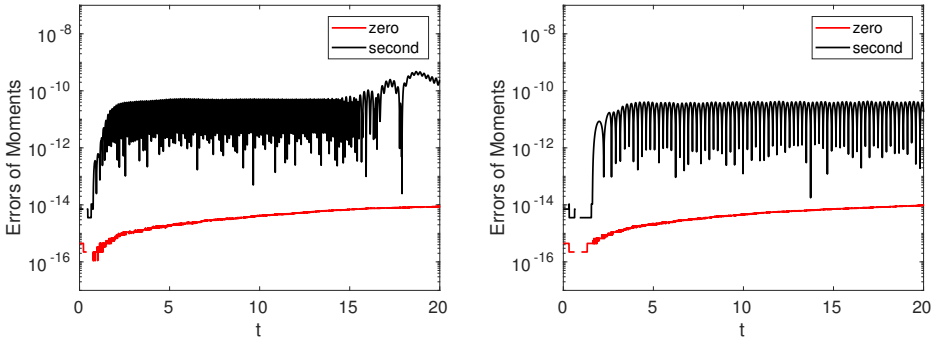

(i) $e = 0.25$ (ii) $e = 0.75$

FIGURE 8. Errors of numerical moments of g from $t = 0$ to $t = 20$.

paper represents our initial effort in solving Boltzmann equations using a spectral basis other than Fourier series.

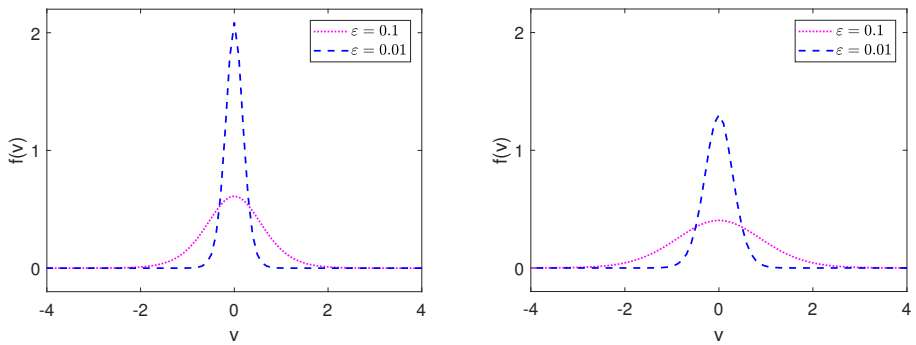

(i) $e = 0.25$ (ii) $e = 0.75$

FIGURE 9. Numerical solutions of heated case at time $t = 20$.

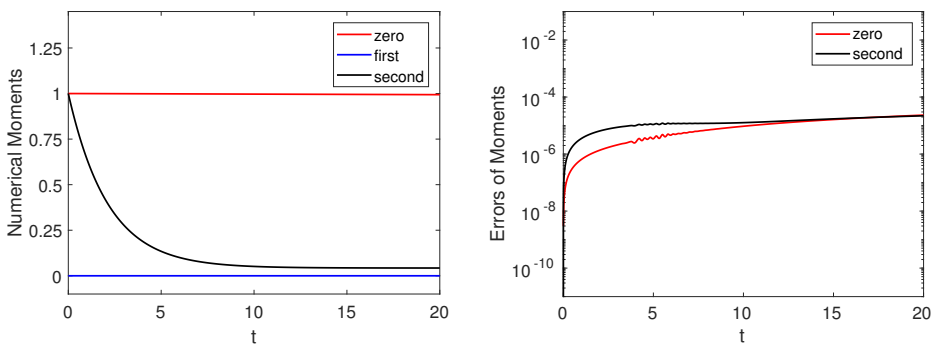

(i) moments (ii) errors

FIGURE 10. Numerical moments of f from $t = 0$ to $t = 20$ with $e = 0.25, \varepsilon = 0.01$.

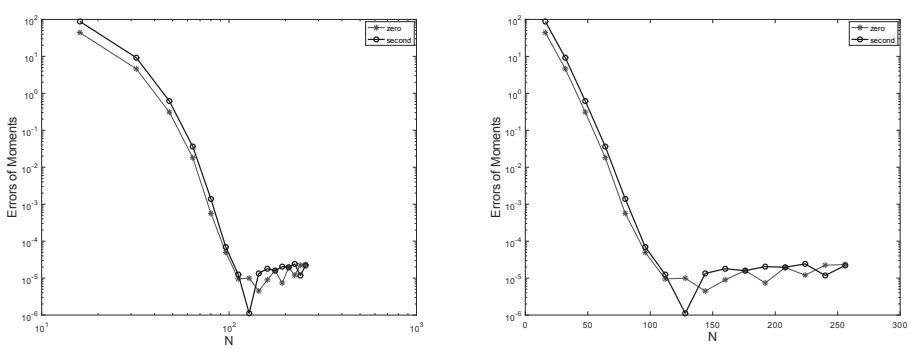

(i) log-log scale (ii) linear-log scale

FIGURE 11. Errors of moments of at $t = 20$ with $e = 0.25, \varepsilon = 0.01$ with respect to different N.

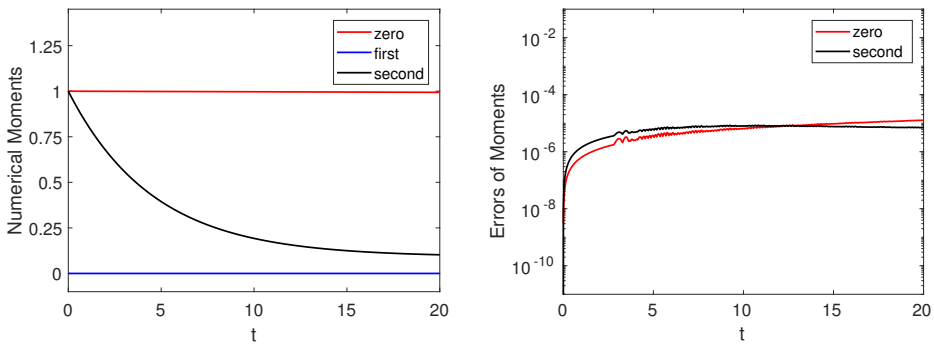

(i) moments (ii) errors

FIGURE 12. Numerical moments of f from $t = 0$ to $t = 20$ with $e = 0.75, \varepsilon = 0.01$.

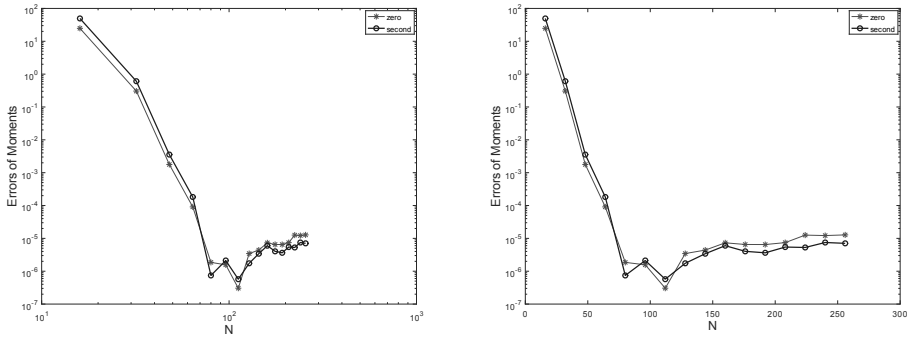

(i) log-log scale (ii) linear-log scale

FIGURE 13. Errors of moments of at $t = 20$ with $e = 0.75, \varepsilon = 0.01$ with respect to different N.

While our discussion is limited to the one-dimensional case in this paper, it is clear that the essential ingredients of the proposed method, mapped Chebyshev functions and the Petrov-Galerkin formulation, can be applied to the multi-dimensional case. However, a feasible implementation in multi-D would require new strategies to compute the collision terms more efficiently.

In the current 1D setting, we first precompute the tensors $\tilde{I}_1(i,j,k)$ and $\tilde{I}_2(i,j,k)$ ($0 \le i,j,k \le N$, where N is the number of expansion in (65)) using the 2D fast Chebyshev transform, hence the pre-computation cost is $O(N^3 \log N)$ and the storage requirement is $O(N^3)$. Then, the numerical complexity to evaluate $\tilde{Q}_k^{e,\lambda}$ for all k is $O(N^3)$. In the multi-dimensional case ($v \in \mathbb{R}^d,\ d = 2,3$), a direct extension of the above approach would require $O(N^{3d} \log N)$ complexity in the pre-computation, with $O(N^{3d})$ storage requirement and $O(N^{3d})$ complexity for evaluation of the collision operator. This quickly becomes a bottleneck when N is large.

We are working on developing a fast algorithm to accelerate the evaluation of the collision operator as well as to alleviate the storage requirement. As a starting

point, we rewrite (67) as:

$$\begin{aligned}\tilde{Q}_k^{e,\lambda} &= \int_{\mathbb{R}}\int_{\mathbb{R}} B_\lambda(|v-w|) f_N(v) f_N(w) \left[\hat{T}_k(v') - \hat{T}_k(v)\right] \mathrm{d}v\,\mathrm{d}w \\ &= \int_{\mathbb{R}} \left(\int_{\mathbb{R}} B_\lambda(|v-w|) f_N(w) \hat{T}_k(v')\,\mathrm{d}w\right) f_N(v)\,\mathrm{d}v \\ &\quad - \int_{\mathbb{R}} \left(\int_{\mathbb{R}} B_\lambda(|v-w|) f_N(w)\,\mathrm{d}w\right) f_N(v) \hat{T}_k(v)\,\mathrm{d}v, \end{aligned} \tag{113}$$

and notice that the inner integral for the gain term can be computed by a nonuniform fast Fourier transform in $O(N \log N)$ operations using similar ideas as proposed in [46, 10]. Together with the outer integral, which has to be evaluated directly, results in a computational cost of $O(N^2 \log N)$. Similar acceleration can be achieved for the loss term. Combining this in a multi-dimensional framework, it is hopeful to arrive at a fast algorithm which can evaluate the collision term in $O(N^{2d} \log N)$ operations and everything will be computed on-the-fly, hence no pre-computation with excessive storage is required.

Acknowledgments. J. Hu would like to thank Ricardo Alonso, Jose A. Carrillo, and Changhui Tan for helpful discussion on inelastic kinetic models. We thank Xiaodong Huang for pointing out the mistakes in a previous version of the paper.

REFERENCES

[1] A. Baldassarri, A. Puglisi, and U. Marconi, Kinetics models of inelastic gases, *Math. Models Methods Appl. Sci.*, **12** (2002), 965–983.

[2] A. Barrat, E. Trizac, and M. H. Ernst, Granular gases: Dynamics and collective effects, *J. Phys.: Condens. Matter*, **17** (2005), S2429–S2437.

[3] D. Benedetto, E. Caglioti, J. A. Carrillo and M. Pulvirenti, *A non-Maxwellian steady distribution for one-dimensional granular media*, *J. Stat. Phys.*, **91** (1998), 979–990.

[4] D. Benedetto and M. Pulvirenti, *On the one-dimensional Boltzmann equation for granular flows*, *M2AN: Math. Model. Numer. Anal.*, **35** (2001), 899–905.

[5] A. V. Bobylev, J. A. Carrillo, and I. M. Gamba, On some properties of kinetic and hydrodynamic equations for inelastic interactions, *J. Statist. Phys.*, **98** (2000), 743–773.

[6] A. V. Bobylev and C. Cercignani, Moment equations for a granular material in a thermal bath, *J. Statist. Phys.*, **106** (2002), 547–567.

[7] A. V. Bobylev and C. Cercignani, Self-similar asymptotics for the Boltzmann equation with inelastic and elastic interactions, *J. Statist. Phys.*, **110** (2003), 333–375.

[8] A. V. Bobylev and S. Rjasanow, *Fast deterministic method of solving the Boltzmann equation for hard spheres*, *Eur. J. Mech. B Fluids*, **18** (1999), 869–887.

[9] J. P. Boyd, *Chebyshev and Fourier Spectral Methods*, $2^n d$ edition, Dover Publications, Inc., Mineola, NY, 2001.

[10] J. Bremer and H. Yang, *Fast algorithms for Jacobi expansions via nonoscillatory phase functions*, preprint, 2018, `arXiv::`1803.03889.

[11] N. V. Brilliantov and T. Pöschel, *Kinetic Theory of Granular Gases*, Oxford University Press, Oxford, UK, 2004.

[12] J. A. Carrillo, C. Cercignani and I. M. Gamba, Steady states of a Boltzmann equation for driven granular media, *Phys. Rev. E*, **62** (2000), 7700–7707.

[13] J. A. Carrillo and G. Toscani, Contractive probability metrics and asymptotic behavior of dissipative kinetic equations, *Riv. Mat. Univ. Parma*, **6** (2007), 75–198.

[14] C. Cercignani, *Recent developments in the mechanics of granular materials*, in *Fisica Matematica e Ingeneria Delle Strutture*, Pitagora Editrice, Bologna, 1995, 119–132.

[15] G. Chai and T.-J. Wang, Generalized hermite spectral method for nonlinear Fokker-Planck equations on the whole line, *J. Math. Study*, **51** (2018), 177–195.

[16] G. Dimarco and L. Pareschi, Numerical methods for kinetic equations, *Acta Numer.*, **23** (2014), 369–520.

[17] F. Filbet, On deterministic approximation of the Boltzmann equation in a bounded domain, *Multiscale Model. Simul.*, **10** (2012), 792–817.

[18] F. Filbet, C. Mouhot and L. Pareschi, Solving the Boltzmann equation in NlogN, *SIAM J. Sci. Comput.*, **28** (2006), 1029–1053.

[19] F. Filbet, L. Pareschi, and G. Toscani, Accurate numerical methods for the collisional motion of (heated) granular flows, *J. Comput. Phys.*, **202** (2005), 216–235.

[20] F. Filbet and T. Rey, A rescaling velocity method for dissipative kinetic equations. Applications to granular media, *J. Comput. Phys.*, **248** (2013), 177–199.

[21] F. Filbet and G. Russo, High order numerical methods for the space non-homogeneous Boltzmann equation, *J. Comput. Phys.*, **186** (2003), 457–480.

[22] I. M. Gamba, J. R. Haack, C. D. Hauck and J. Hu, A fast spectral method for the Boltzmann collision operator with general collision kernels, *SIAM J. Sci. Comput.*, **39** (2017), B658–B674.

[23] I. M. Gamba, V. Panferov, and C. Villani, On the Boltzmann equation for diffusively excited granular media, *Commun. Math. Phys.*, **246** (2004), 503–541.

[24] I. M. Gamba and S. Rjasanow, Galerkin-Petrov approach for the Boltzmann equation, *J. Comput. Phys.*, **366** (2018), 341–365.

[25] I. M. Gamba, S. Rjasanow and W. Wagner, Direct simulation of the uniformly heated granular Boltzmann equation, *Math. Comput. Modelling*, **42** (2005), 683–700.

[26] I. M. Gamba and S. H. Tharkabhushanam, Spectral-Lagrangian methods for collisional models of non-equilibrium statistical states, *J. Comput. Phys.*, **228** (2009), 2012–2036.

[27] J. Hu and Z. Ma, A fast spectral method for the inelastic Boltzmann collision operator and application to heated granular gases, *J. Comput. Phys.*, **385** (2019), 119–134.

[28] J. Hu and L. Ying, A fast spectral algorithm for the quantum Boltzmann collision operator, *Commun. Math. Sci.*, **10** (2012), 989–999.

[29] G. Kizler and J. Schröberl, A polynomial spectral method for the spatially homogenenous Boltzmann equation, *SIAM J. Sci. Comput.*, **41** (2019), B27–B49.

[30] J. C. Mason and D. C. Handscomb, *Chebyshev Polynomials*, Chapman and Hall/CRC, Boca Raton, FL, 2003.

[31] C. Mouhot and L. Pareschi, Fast algorithms for computing the Boltzmann collision operator, *Math. Comp.*, **75** (2006), 1833–1852.

[32] G. Naldi, L. Pareschi and G. Toscani, Spectral methods for one-dimensional kinetic models of granular flows and numerical quasi elastic limit, *M2AN Math. Model. Numer. Anal.*, **37** (2003), 73–90.

[33] L. Pareschi and B. Perthame, A Fourier spectral method for homogeneous Boltzmann equations, *Transport Theory Statist. Phys.*, **25** (1996), 369–382.

[34] L. Pareschi and G. Russo, Numerical solution of the Boltzmann equation I. Spectrally accurate approximation of the collision operator, *SIAM J. Numer. Anal.*, **37** (2000), 1217–1245.

[35] L. Pareschi and G. Toscani, *Interacting Multiagent Systems*, Oxford University Press, UK, 2014.

[36] S. Rjasanow and W. Wagner, Time splitting error in DSMC schemes for the spatially homogeneous inelastic Boltzmann equation, *SIAM J. Numer. Anal.*, **45** (2007), 54–67.

[37] J. Shen, T. Tang, and L.-L. Wang, *Spectral Methods: Algorithms, Analysis and Applications*, Springer-Verlag, Berlin-Heidelberg, 2011.

[38] J. Shen, L.-L. Wang and H. Yu, Approximations by orthonormal mapped Chebyshev functions for higher-dimensional problems in unbounded domains, *J. Comput. Appl. Math.*, **265** (2014), 264–275.

[39] G. Toscani, One-dimensional kinetic models of granular flows, *M2AN Math. Model. Numer. Anal.*, **34** (2000), 1277–1291.

[40] T. P. C. van Noije and M. H. Ernst, Velocity distributions in homogeneous granular fluids: The free and the heated case, *Granular Matter*, **1** (1998), 57–64.

[41] C. Villani, Mathematics of granular materials, *J. Stat. Phys.*, **124** (2006), 781–822.

[42] Y. Wang and Z. Cai, Approximation of the Boltzmann collision operator based on Hermite spectral method, *J.Comput. Phys*, **397** (2019), 108815, 23 pp.

[43] D. Williams and F. Mackintosh, Driven granular media in one dimension: Correlations and equation of state, *Phys. Rev. E*, **54** (1996), R9–R12.

[44] L. Wu, C. White, T. J. Scanlon, J. M. Reese and Y. Zhang, Deterministic numerical solutions of the Boltzmann equation using the fast spectral method, *J. Comput. Phys.*, **250** (2013), 27–52.

[45] L. Wu, Y. Zhang and J. M. Reese, Fast spectral solution of the generalized Enskog equation for dense gases, *J. Comput. Phys.*, **303** (2015), 66–79.

[46] H. Yang, A unified framework for oscillatory integral transform: When to use NUFFT or butterfly factorization, *J. Comput. Phys.* **388** (2019), 103–122.

[47] X. Yu, Y. Zhao and Z. Wang, A diagonalized Legendre rational spectral method for problems on the whole line, *J. Math. Study*, **51** (2018), 196–213.

Received June 2019; revised January 2020.

E-mail address: jingweihu@purdue.edu
E-mail address: shen7@purdue.edu
E-mail address: Yingwei.Wang@sas.com